AD-A091 512 NAVAL ACADEMY ANNAPOLIS MD F/G 13/10
THE EFFECTS OF VOYAGING ON THE MAGNETIZATION OF SHIP MODELS.(U)
MAY 80 E A BELZER
UNCLASSIFIED USNA-TSPR-104 NL

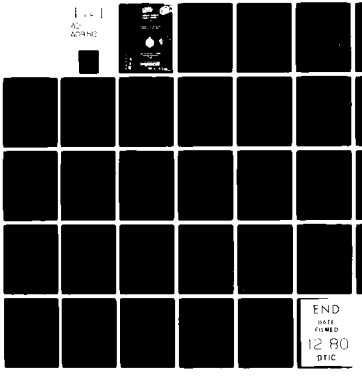

END
DATE FILMED
12 80
DTIC

UNCLASSIFIED

SECURITY CLASSIFICATION OF THIS PAGE (When Data Entered)

REPORT DOCUMENTATION PAGE		READ INSTRUCTIONS BEFORE COMPLETING FORM
1. REPORT NUMBER U.S.N.A. - TSPR; no. 104 (1980)	2. GOVT ACCESSION NO. AD-A092	3. RECIPIENT'S CATALOG NUMBER 512
4. TITLE (and Subtitle) THE EFFECTS OF VOYAGING ON THE MAGNETIZATION OF SHIP MODELS.		5. TYPE OF REPORT & PERIOD COVERED Final: 1979/1980
		6. PERFORMING ORG. REPORT NUMBER
7. AUTHOR(s) Elizabeth Anne Belzer		8. CONTRACT OR GRANT NUMBER(s) Final rept. 1979-1980.
9. PERFORMING ORGANIZATION NAME AND ADDRESS United States Naval Academy, Annapolis.		10. PROGRAM ELEMENT, PROJECT, TASK AREA & WORK UNIT NUMBERS 12 59
11. CONTROLLING OFFICE NAME AND ADDRESS United States Naval Academy, Annapolis.		12. REPORT DATE 5 May 1980 13. NUMBER OF PAGES 55
14. MONITORING AGENCY NAME & ADDRESS(if different from Controlling Office) USNA-TSPR-104		15. SECURITY CLASS. (of this report) UNCLASSIFIED 15a. DECLASSIFICATION/DOWNGRADING SCHEDULE

16. DISTRIBUTION STATEMENT (of this Report)

This document has been approved for public release; its distribution is UNLIMITED.

17. DISTRIBUTION STATEMENT (of the abstract entered in Block 20, if different from Report)

This document has been approved for public release; its distribution is UNLIMITED.

18. SUPPLEMENTARY NOTES

Accepted by the U. S. Trident Scholar Committee.

19. KEY WORDS (Continue on reverse side if necessary and identify by block number)

Voyaging
Magnetization
Cyclic stress
Vibration
gauge

20. ABSTRACT (Continue on reverse side if necessary and identify by block number)

The effects of voyaging on the magnetization of ship models were tested by subjecting two sample rods, one of HY100 steel and one of HY130 steel to an apparatus for supply of cyclic stress of two amplitudes, approximately fifty and one hundred microstrains, as measured by resistance to strain guage bridges. A circuit was built to measure changes in magnetic induction. Results showed an increase in initial susceptibility for both rods. HY130 proved more susceptible than HY100 in all cases. The Rayleigh coefficient was measured for each

OVER !

DD FORM 1 JAN 73 1473 EDITION OF 1 NOV 65 IS OBSOLETE

S/N 0102-LF-014-6601

UNCLASSIFIED

SECURITY CLASSIFICATION OF THIS PAGE (When Data Entered)

245600

20. CONTINUED:

steel, and these were compared with the slope of the normal susceptibility with strain amplitude to determine the fracture of domains responsive to stress. An increase in magnetization in the presence of a field, related to the log of the number of cycles, was observed. The change of the magnetization with the first cycle of stress was found to be large in comparison to changes which occurred through subsequent cycles. Continuation of vibration for several months is now seen as adequate to produce comparable first cycle and long-term effects. Thus, a model for changes in magnetization of Navy ships with time has been established.

0 - 0

THE EFFECTS OF VOYAGING ON THE MAGNETIZATION OF SHIP MODELS

A Trident Scholar Project Report

by

Midshipman Elizabeth A. Belzer, Class of 1980
U. S. Naval Academy
Annapolis, Maryland

Carl S. Schneider

Advisor: Assoc. Prof. Carl S. Schneider
Physics Department

Accepted for Trident Scholar Committee

Chairman

5 May 1980

Date

ABSTRACT

Two sample rods, one of HY100 steel and the other of HY130 steel, were tested as to the effects on susceptibility and magnetization of cyclic stress. An apparatus was built for applying cyclic stress of two amplitudes, approximately fifty and one hundred microstrains, as measured by resistance strain gage bridges. A circuit was built to measure changes in magnetic induction using an induction coil and a magnetometer probe. Results showed an increase in initial susceptibility for both rods, as well as an increase in the change in susceptibility with increasing field in the presence of cyclic stress. The HY130 sample's susceptibility was higher than that of the HY100 in all cases. The slope of the normal susceptibility with field, or Rayleigh coefficient, was measured for each steel, and these were compared with the slope of the normal initial susceptibility with strain amplitude to determine the fraction of domains responsive to stress. The calculated value of this fraction was .55.

In addition, long-term effects of cyclic stress on magnetization were studied. An increase in magnetization in the presence of a field, related to the log of the number of cycles, was observed. The change of the magnetization with the first cycle of stress was found to be large in comparison to changes which occurred through subsequent cycles. Continuation of vibration for several months is now seen as adequate to produce comparable first cycle and long-term effects. Thus, a model for changes in magnetization of Navy ships with time has been established.

ACKNOWLEDGMENTS

A great deal of credit must be given to those individuals without whom the year's work would not have been worthwhile. Their time and effort provided the framework for the success of this project.

First, my deepest respect and appreciation goes to Professor Carl S. Schneider, for without his knowledge and perseverance this work could not have been completed. I would like to thank those individuals in the Physics and Engineering departments who built the apparatus used and helped work out all the mechanical problems encountered. In addition, I would like to thank Captain Robert J. Kimble, USMC, for the computer program which made graphical data analysis possible. Finally, I would like to thank my mother, Mrs. Esther L. Belzer, and my fiance', Ensign John H. Semcken, III, USN, for their never ending support.

Elizabeth A. Belzer

Elizabeth A. Belzer USNA '80

PREFACE

The research included in this report is a contribution to Project Linear Chair, originating at the David W. Taylor Naval Ship Research and Development Center. One objective of that project is to develop methods by which the magnetization changes of a ship during turns, dives, and voyaging may be predicted and through this, methods for compensation produced.

The objective of this project has been to concentrate on the area of voyaging or, in other words, movements of the ship other than turns and dives. In particular, the area of vibration is dealt with; vibrations caused by shipboard machinery, waves and the like.

Prior to this research, the effects of static stress had already been investigated, with the result that magnetization changes were produced by varying strain and magnetic field intensity applied to steel rods. Results from this project, then, will show the changes in permeability and magnetization in ship steels produced by cyclic stress (vibration) in the presence of magnetic fields.

TABLE OF CONTENTS

INDEX TO FIGURES*

*Numbers in parentheses refer to reference used, if any.

CHAPTER I

BACKGROUND

The objective of this project was to discover and measure the changes in magnetization of ship steels due to vibration. If these changes can be predicted, it may be possible for a ship to perform certain maneuvers which could bring the ship to a well-known magnetic state, thereby making its magnetization controllable.

The effects addressed within this paper are those due to voyaging, including those related to internal machinery and external waves, as well as those related to lightning, violent sea states or collisions. Voyaging includes all magnetic effects on a seagoing vessel other than those from diving.

There are two types of voyage effects. The first is thermal relaxation, which will be addressed briefly. The second, and the one with which this project deals, is those effects which are of an environmental nature; specifically, those effects due to vibration. Both of these voyage effect types are very much time-dependent, with time constants ranging from seconds to months to years. This project addresses only relatively short time periods, with indications for extrapolation to much longer periods.

The effect of vibration in a weak field, such as

that of the earth, was demonstrated by Gilbert nearly 400 years ago. A bar of iron was magnetized by hammering it while in the presence of the earth's magnetic field. The magnetism remained after the bar was removed from the earth's field unless the magnetism was removed by more tapping or by applying a stronger magnetic field of the opposite sign (1). A steel ship, then, is magnetized in a similar manner when it is built. The last "in-depth" research in the field of vibration magnetics was published in 1892 by Ewing. His premise was that vibration of soft iron decreases the hysteresis effects normally observed (1). In order to have an understanding of this theory, the magnetization process must first be explained.

First, consider an unmagnetized sample of ferromagnetic material. If the magnetic intensity, H, is increased from zero, the magnetic induction, B, will increase as well. The B vs. H curve created by this process is called the magnetization curve of that particular material. If the magnetic intensity, H, is then decreased to zero, the B vs. H curve does not follow the curve originally established. A reversed or negative magnetic intensity is necessary to reduce the magnetic induction to zero. By increasing H in the reverse direction, a symmetry with that in the positive direction is established. When H is again increased in the forward direction, a loop is completed. This entire process is

shownin Figure 1 (2). This, then, is what Ewing refers to as the hysteresis curve, the word hysteresis coming from the Greek word meaning "to lag." In other words, magnetic induction lags the applied field (3).

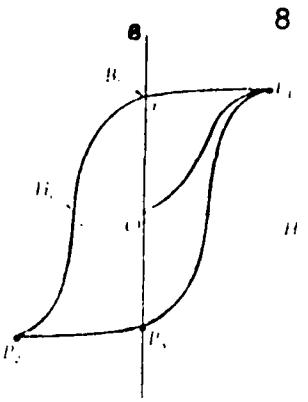

Figure 1: B versus H for hard ferromagnetic material. The outer curve is called a hysteresis curve.

The maximum value of the B-field shown in the figure indicates saturation magnetization, M_s, and the negative field required to bring the induction back to zero after applying that field is called the coercive force, H_c (2). The coercive force for the ship steels used for these experiments is approximately 9.3 oersteds. The graphical results also show that the B vs. H curve for increasing magnetic intensity is entirely different from the B vs. H curve for decreasing magnetic intensity.

Ewing found that if a piece of soft iron was tapped during the application and removal of a magnetizing force, the susceptibility, or increase in magnetic moment caused by the application of a field, increased when the field was applied. When the field was removed, the tapping reduced the ability of the iron to retain the magnetization. In other words, the vibration allowed the magnetic domains more freedom of movement than they normally have (1). Vibration, then, makes the steel respond more easily

to processes which tend to change its magnetization.

Many years ago, this phenomenon was described on a molecular level, stating that vibration produces periodic displacement of molecular centers, thereby causing the "molecular magnets" to oscillate. This effect allows the molecules periodic freedom of movement. If an external field, such as that of the earth, is then applied, the molecules yield more readily to it during the moments of freedom, and residual magnetism is reduced. This description is helpful in depicting the types of processes which occur, but it is now known that magnetic domains, rather than molecules, are responsible for the changes described. The effect mentioned above may occur even in the absence of an external field, although it is slight (2).

Ewing proposed that by removing residual magnetism, or remanence, which is that amount of magnetic induction remaining after the H-field is decreased to zero (see Figure 1), the vibration acts first in small areas, such that remanence is decreased in this area. This area, then, produces a demagnetizing field around itself. In a similar manner, the demagnetization of a long iron rod begins at the ends, where there is a self-demagnetizing field, and then moves toward the center (1). Ewing's predictions, however, were only qualitative. In this paper, experimental analysis of these effects will be presented.

Although little work has been done during the 20th century in the area of vibration effects on magnetism, much research <u>has</u> been done in the area of static stress

effects on metals, including steel, as well as the magnetic equivalency of mechanical stresses and applied fields. In order to have an understanding of the methods used for the analysis of vibration effects, it is necessary to become familiar with the concepts behind prior research.

In the 1940's William F. Brown, Jr., performed research at the Naval Ordnance Laboratory concerning stress effects on magnetization. It was found that when a steel specimen is magnetized at a small magnetizing force H, and then subjected to a small tension cycle, magnetization increases upon application. This increase is proportional to the slope of the permeability, μ, vs. H curve (see Figure 2, next page) (4), and remains at the new value when tension is removed (5).

Brown found that stresses which affect ships are magnetically equivalent to small fields. This analysis is determined by the theory of domain wall displacements. This theory indicates that jumps of "walls" within metals respond to various amounts of magnetic force or stress.

The domains present within a specimen are induced by the strain of grinding the surface during formation. The size of the domains is independent of the shape of the specimen, and the stable domain structure is formed in a manner which minimizes the total energy of the specimen. For example, in cylindrical iron or steel specimens, such as those used in this experiment, the magnetization averaged over the x, y and z domains points parallel to the

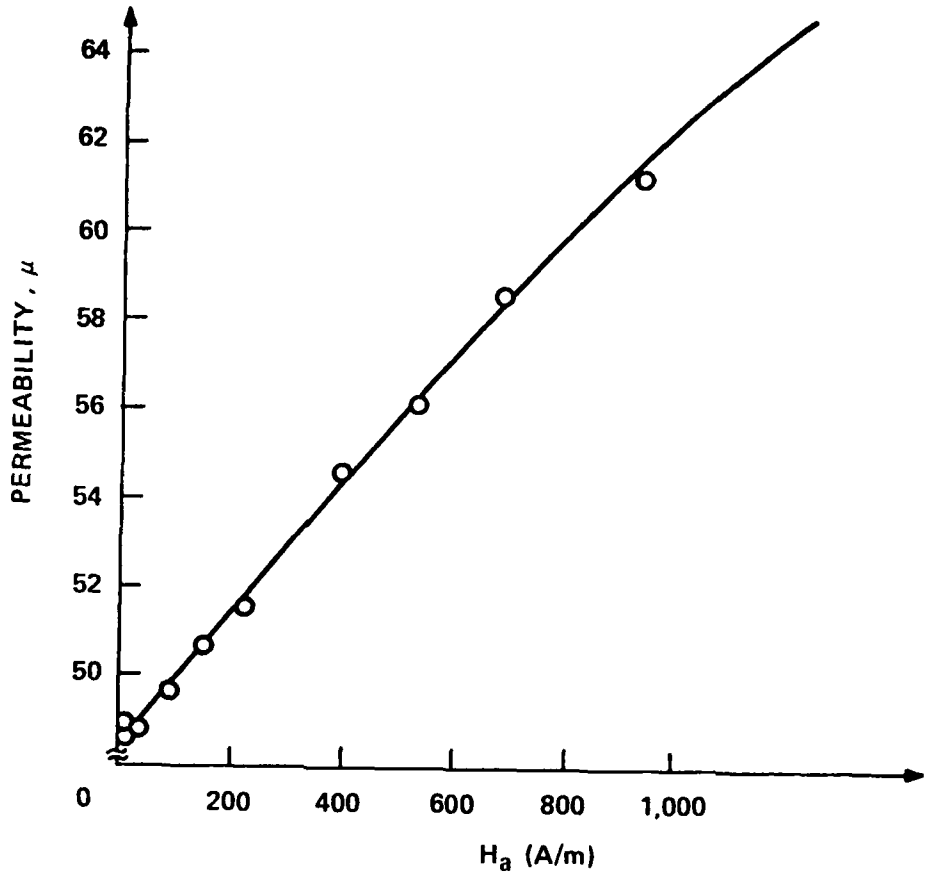

Figure 2 -- Apparent Permeability Versus Applied Field

long axis of the specimen, because the normal component of magnetization would otherwise induce free poles on the side surface, giving rise to a large magnetostatic energy. This energy is defined as the energy due to the Coulomb-like ($1/r^2$) interaction between magnetic free poles and tends to be minimized, as stated above, at equilibrium (2).

Brown investigated the theory of domain wall displacement in the following manner. A rod made of soft iron or steel has field, tension, or both

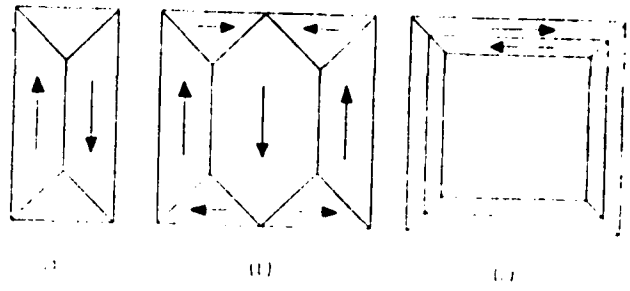

Figure 3 -- [illegible]

applied uniformly along its axis. The specimen consists of crystals with randomly oriented axes. The crystal domains, then, are saturated along one of the "directions of easy magnetization" for demagnetization; in other words, in the [100] direction (5). This implies that there are six "easy" directions for cubic crystals. Therefore, a field of 1 öersted or less is required to change magnetization along these directions, while a field of approximately 500 öersteds is required along, for example, the [111] direction. Noting this, there is obvious anisotropy in the energy necessary for magnetizing the crystal in a given direction (6).

In addition, the more favorably magnetized domain, which is the domain whose magnetization vector is closer in direction to the tension or magnetic force, grows at the expense of its neighbor. There are three types of domain walls. 180° walls are those with spins which rotate 180° in passing from one domain to the next one. Similarly, 90° walls are those which rotate 90° in passing from one domain to the next. There are two types of 90° walls, however, positive and negative, each rotating in the opposite direction (see Figure 3) (2).

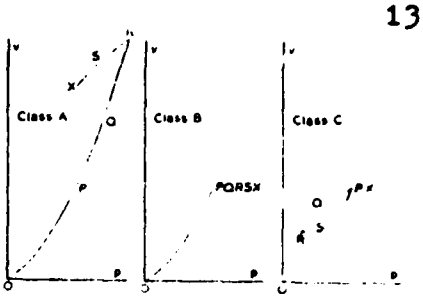

Average behavior of a group of walls of one type. Class *A*, 90° walls for which tension is equivalent to positive magnetizing force; Class *B*, 180° walls; Class *C*, 90° walls for which tension is equivalent to negative magnetizing force. *OP*, magnetizing force applied; *PQR*, tension applied; *RSX*, tension removed. Abscissa *p* is hydrostatic pressure to which magnetizing force and tension are equivalent; ordinate *v* is volume swept out by walls of the specified type in unit volume of the specimen.

Figure 4 -- Average behavior of Domain Wall Types

90° walls indicate, then, the more favorable magnetized domains and can therefore be displaced by tension or magnetic force, while 180° walls are unaffected. Furthermore, both reversible and irreversible displacements of 90° walls are observed. Figure 4 shows the three domain wall types divided into classes:

Class A -- displacement of the same sign under positive tension ($90^{\circ}+$)

Class B -- unaffected by tension (180°)

Class C -- displacement of the opposite sign under positive tension ($90^{\circ}-$)

In the figure, tension is equated with hydrostatic pressure and the effect on domain wall displacements is represented graphically for each class of wall. The reversible part of the magnetization for the Class A and C walls is $\chi_o H$, where χ_o is the initial susceptibility and H is the applied field. The removal of the tension causes no change in the susceptibility. For this project, the change in susceptibility for repeated tension cycles and the irreversible part of the magnetization are measured.

In Brown's research, it was found that the first of a series of equal shocks, either magnetic or

mechanical, produces 90% or more of the total change in magnetic induction (ΔB) in varying fields. In the small field range, Brown hypothesized that the first shock would produce 100% of the change, but no quantitative data has been found (5).

The results of this previous research, then, can be used to roughly estimate the effects on a ship when it is subjected to normal mechanical disturbances. However, the earth's field experienced by a ship's steel is within the small field range. Therefore, quantitative analysis of the effects of stress cycles in this small field range is needed and is addressed in this report.

Brown states that in the case of a specimen with a negligible and constant demagnetizing field, with the specimen initially demagnetized, the initial rate of rise of induction depends on the frequency of shocks of all amplitudes. The final value is approached asymptotically and is dependent solely on the frequency of the largest shocks. In this project, frequency-dependence will be analyzed for repeated stress cycles of small amplitude, rather than for what Brown refers to as shock (5).

In 1957, Néel addressed the effects of repeated field cycles. His theoretical calculation of these effects was confirmed experimentally by Van Dang in 1959 (7). The theory states that a sequence of increasing and decreasing fields always causes hysteresis loss. The principles which govern the changes caused by this process are Rayleigh's Laws. These laws are only applicable within the Rayleigh region.

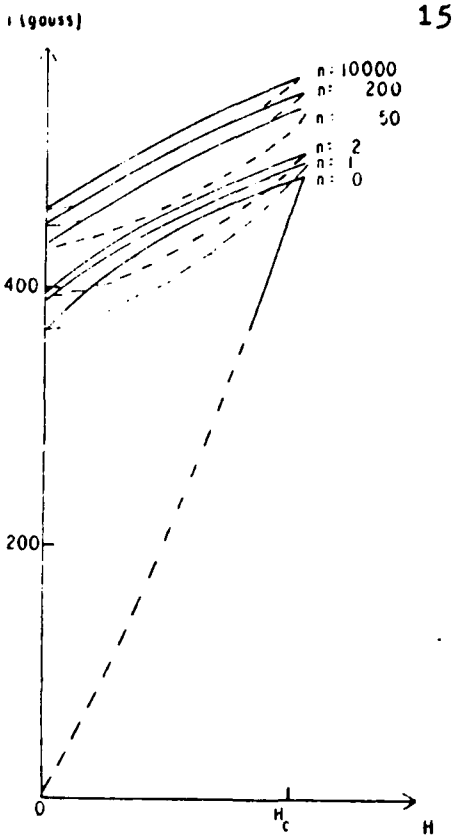

Magnetization curve obtained by Van Dang [13] for a wire illustrating reptation during n cycles at a constant temperature of 17°C

Figure 5 -- Magnetization curve

This is the region where the maximum magnetic field applied is less than approximately one-third of the coercive force, H_c.

However, when H is of the order of H_c, it is found that changes in magnetization become dependent on the number of cycles. Figure 5 shows the effects of cycling "n" times between H=0 and H=H_c for a steel specimen. This particular steel specimen had a coercive force of 13.8 öersteds (6,7).

The main effect is that for large n, both ends of the loop move together to a higher magnitude of magnetization with a $(\log n)^{\frac{1}{2}}$ dependence, derived by Néel (8). This process is called "reptation" or "creeping." Reptation was found to be very small for cycles of amplitude less than $\frac{1}{2}H_c$ and was assumed to be negligible for fieldswithin the Rayleigh region. In this report, the effects of stress cycles as opposed to field cycles are discovered. Similar results again indicate the equivalent effects of

stress and field (6).

The final area to be addressed is that of time effects. Charles Kittel's "theory of long period magnetic relaxation" was developed through experiments using a mild steel specimen subjected to various stresses while in a weak magnetic field of approximately 0.5 Gauss. When the applied field is changed, the magnetization changes in proportion to the susceptibility and demagnetization coefficient of the specimen (9). However, a certain amount of time is required for the magnetization to reach its final state. This lag has been called "magnetic viscosity," "magnetic after-effect" and "Nachwirkung" (15). This effect is associated with the rapid migration of impurities within the steel in the presence of an applied field and thermal oscillations (10).

Two of the time constants Kittel discovered were of the order of three months and five years. These are important for analysis of magnetization changes in ships, but are not analyzed in this work due to time constraints. However, Kittel also discovered that there are magnetic relaxation effects in iron with time constants of minutes or less, with which this project deals (9).

As stated earlier, when an H-field is applied, pressure is exerted on domain walls by strains at wall boundaries. As the internal resistance or opposition to this force relaxes with time, the wall slowly moves further out, increasing the macroscopic magnetization to the equilibrium position. This process may occur to its completion, as Kittel states, in any period of time from seconds to years,

with the majority of the change occurring in a relatively short time (9).

Snoek, who also studied time effects, found that at low temperatures (room temperatures) and under ordinary conditions, the changes which are time-dependent are not detected because they occur too quickly. In addition, through magnetization, any changes in susceptibility are nullified and the susceptibility returns to its original value (11). One objective of this work, then, was to see if any of these time effects could be observed during or after the experiments conducted.

The purpose of this section has been to introduce the reader to the many aspects of magnetization which contribute to the voyage effect, and to summarize the work completed in this field up to the present time. Little quantitative or experimental analysis is available in the area of cyclic stress in small fields, and this project investigates that subject. Research in this area is vitally important for analyzing changes in the magnetization of naval vessels with time.

II. THEORY

During FY1978, in conjunction with the David W. Taylor Naval Ship Research and Development Center, Annapolis, measurements were made to determine the relationship between induced and permanent magnetization, in sample rods made of ship steels, due to changes in applied magnetic field, H_a, and static strain, ϵ, along the sample axis. The theory used for these tests is the same as that used for the present work(4), with some additions.

2-1 Field, Susceptibility and Induction

For the experiments, a current passes through the coils of an end-compensated solenoid enclosing HY100 and HY130 steel sample rods. The field applied, which is uniform within one per cent over the sample, is equivalent to that of an infinite solenoid with a single layer of the same diameter wire(4):

$$H_a = i/d \qquad 2\text{-}1$$

where i is the current and d is the diameter of the H-coil wire.

The field within the sample is decreased from the field, H_a, created by the solenoid by the demagnetizing field, H_D, where:

$$H_D = DM \qquad 2\text{-}2$$

where D is the geometrically determined demagnetization factor of our rods(approximately 1/400) and M is the magnet-

ization density within the sample.

The magnetic induction, B, can be expressed in terms of the net field, H, where:

$$H=H_a-H_D \qquad 2\text{-}3$$

and the material relative permeability, μ, defined below, or in terms of the applied field, H_a, and the effective permeability, μ_{eff}:

$$B=\mu\mu_0 H=\mu_{eff}\mu_0 H_a \qquad 2\text{-}4$$

Since,

$$B=\mu_0(H+M), \qquad 2\text{-}5$$

the component of magnetic induction due to the magnetization density, M, can be expressed in a form similar to equation 2-4:

$$M=\chi_{eff}H_a=\chi H \qquad 2\text{-}6$$

where χ_{eff} is the sample susceptibility and χ is the material susceptibility. It follows that:

$$\mu_{eff}=\chi_{eff}+1 \qquad 2\text{-}7$$

and,

$$\mu=\chi+1. \qquad 2\text{-}8$$

From equations 2-2 and 2-4:

$$H=H_a-DM \qquad 2\text{-}9$$

and from equation 2-6:

$$H=H_a(1-\chi_{eff}D). \qquad 2\text{-}10$$

Therefore, from equations 2-4 and 2-10:

$$\mu = \mu_{eff}H_a/H = \mu_{eff}/(1-\chi_{eff}D), \qquad 2\text{-}11$$

and thus, the material susceptibility is:

$$\begin{aligned}\chi &= \mu - 1 = (\chi_{eff}+1)/(1-\chi_{eff}D)-1 \\ &= \chi_{eff}(1+D)/(1-\chi_{eff}D) \qquad 2\text{-}12\end{aligned}$$

where for our rods $D \ll 1$ and therefore:

$$\chi \cong \chi_{eff}/(1-\chi_{eff}D). \qquad 2\text{-}13$$

The induction, B, of the sample is sensed with a pick-up coil around the sample rods, which are centrally positioned within the H-coil. Because the B-coil wire is wound around the samples themselves, no airgap correction is necessary. From Faraday's law, a change of flux, ϕ, in the B-coil produces a voltage:

$$V_B=N_B(d\phi/dt) \qquad 2\text{-}14$$

where N_B is the number of turns of wire around the sample steel rods. This voltage is integrated, and therefore, the change in flux is calculated in the following manner:

$$d\phi/dt \cong A\,\mu_0 M/RC \qquad 2\text{-}15$$

where,

A=B-coil pick-up area
μ_0=permeability of free space
M=residual magnetization density
RC=integrator time constant determined by a fixed capacitor, C, and a variable resistor, R.

Using equations 2-6, 2-14 and 2-15, the effective permeability can be calculated using the definition of the magnetization density:

$$M \cong \mu_{eff} H_a = RCV_B / N_B \mu_0 A \qquad 2\text{-}16$$

and therefore:

$$\mu_{eff} = RCV_B / N_B \mu_0 A H_a . \qquad 2\text{-}17$$

It follows from equation 2-7 that the sample susceptibility is:

$$\chi_{eff} = (RCV_B / N_B \ \ _0 A H_a) - 1 . \qquad 2\text{-}18$$

Using this equation and equation 2-13, the material susceptibility can be calculated for the experiments.

2-2 Strain Gages

In order to measure strain, strain gages were applied directly to the rods. A strain gage may be considered to be a pattern of N fine rods of length L, width w and thickness t, connected by fat rods of negligible resistance. The resistance is calculated to be:

$$R = \rho NL / wt \qquad 2\text{-}19$$

where ρ is the resistivity of the strain gage material.

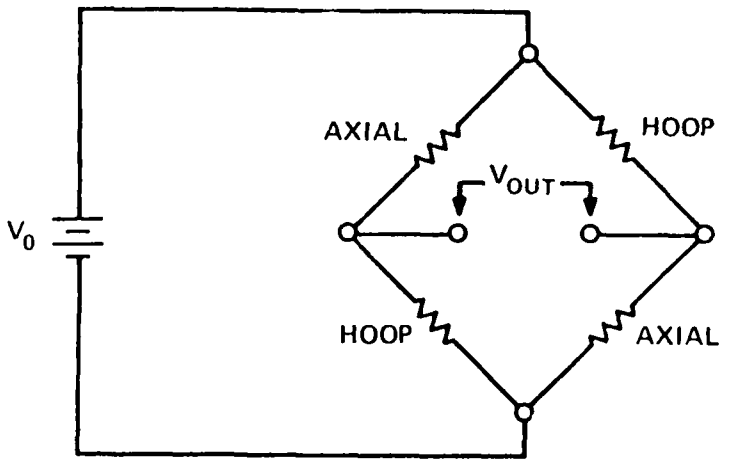

Figure 6--Strain Bridge Circuit Diagram

When the gage is strained, its dimensions become:

$$\begin{aligned} &(a)\quad L'=L(1+\epsilon) \\ &(b)\quad w'=w(1-\sigma_p\epsilon) \\ &(c)\quad t'=t(1-\sigma_p\epsilon) \end{aligned} \qquad 2\text{-}20$$

where ϵ is the axial strain and σ_p is Poisson's ratio. Thus, for small changes:

$$\begin{aligned} \Delta R/R &= (\Delta L/L)-(\Delta w/w)-(\Delta t/t)+(\Delta\rho/\rho) \\ &= \epsilon(1+2\sigma_p)=\epsilon F_g \end{aligned} \qquad 2\text{-}21$$

where F_g is the strain gage factor(13).

Since the resistance change is approximately a part per million for microstrain measurements, a Wheat stone bridge is used for these measurements(see Figure 6). Two axial gages and two hoop gages are mounted on opposite sides of the cylindrical samples and wired such that the transverse strain associated with Poisson's ratio increases the offset voltage from hoop stress, but cancels voltages from bending. The resulting bridge

factor, which is defined by the equation for strain-induced offset voltage:

$$\Delta V = V_0 F_{br} F_g \epsilon \qquad 2\text{-}22$$

where V_0 is the externally applied DC voltage and F_{br} is the bridge factor, is then(17):

$$F_{br} = (1+\sigma_\rho)/2. \qquad 2\text{-}23$$

When the rod undergoes strain along the axis, the effects of bending must be considered. Bending creates a torque causing large local strains, which may adversely affect the correlation of strain with strain effects. It is found, however, that as long as the rod is not buckling, the bending effect is much less than the uniaxial strain measured by the gages and therefore needs not be considered.

2-3 Rayleigh's Theory

The theory which most directly relates to the objective of this project comes from Rayleigh's theory. Rayleigh investigated the changes in susceptibility due to applied fields within the Rayleigh region($< 1/3\ H_c$). His plot of susceptibility vs. H-field is similar to the permeability vs. H curve of Figure 2(see Figure 7, next page). Here, differential susceptibility is defined as the change in magnetization with change in field. Because of this, the area under the curve, or the integral of the susceptibility, is the change in magnetization. The effective field due to stress and field is:

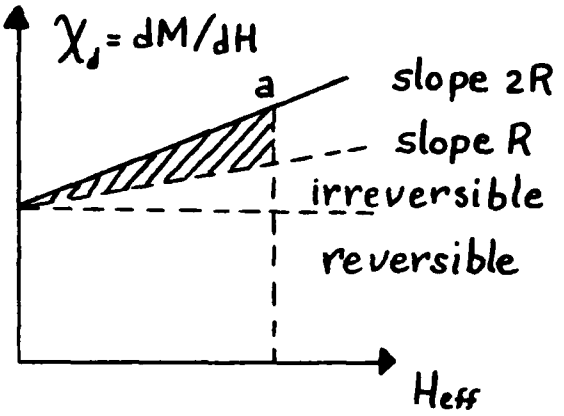

Figure 7

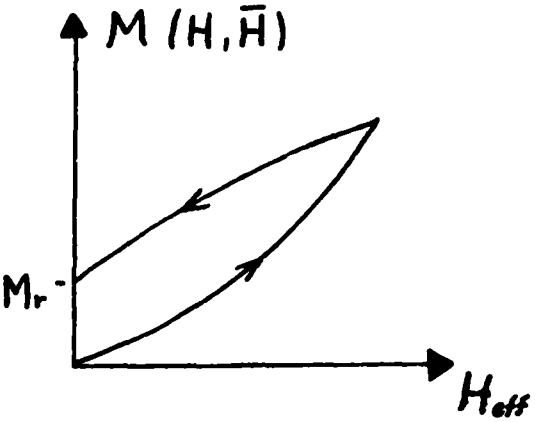

Figure 8

$$H_{eff}=H_a \pm H_\epsilon \qquad 2\text{-}24$$

where H_a is the applied magnetic field and H_ϵ is the effective field due to stress. This means, then, that applied stress is equivalent to a field in its effect on magnetization and susceptibility(14). According to energy density(10):

$$\mu_0 M_s H_\epsilon = (3/2)\lambda_s \epsilon Y \qquad 2\text{-}25$$

where M_s is the saturation magnetization and λ_s is the saturation magnetostriction and Y is Young's Modulus.

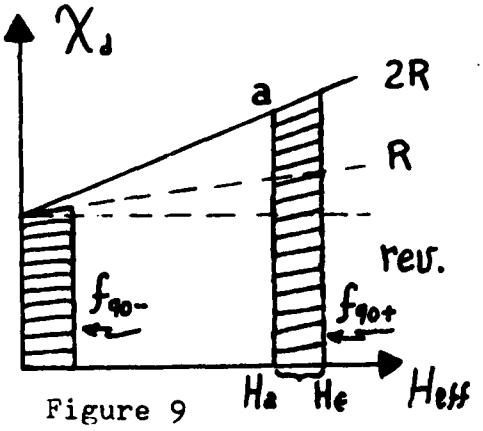

Figure 9

Figure 7 shows that when the field increases, the susceptibility increases linearly. If, at point a, the effective field is then decreased, theory states that the magnetization decreases by the area under a curve which begins

at H=0 and increases with a slope of one-half that from the originally applied field. The initial slope is 2R, where R is Rayleigh's coefficient, and the reduced slopeis, as stated, one-half of that or R. Thus, all of the "reversible" magnetization is lost upon removing the field H, while half of the "irreversible" magnetization is lost, leaving a magnetization at zero field called "remanent magnetization," M_r.

The resulting M vs. H curve is shown in Figure 8(previous page). Here we see a hysteresis curve and the remanent magnetization due to H. The reduction by one-half in curvature as the field is reduced is also apparent. The remanent magnetization was derived by Rayleigh to be:

$$M_r = \tfrac{1}{2}RH^2. \qquad 2\text{-}26$$

If,after applying a field, stress is also applied, the 180 degree domain walls are not affected as stated earlier. The 90 degree(+) and 90 degree(-) walls are affected, but in different ways. The 90 degree(+) walls experience an increased field; the 90 degree(-) walls, however, change on magnetization as if the field were being decreased, or a negative field were being applied. The result, then, is just as was described earlier; the 90 degree(+) walls add to the magnetization with a continuing slope of 2R, while the 90 degree(-) walls reduce the magnetization beginning again at H=0 with a slope of R, as shown in Figure 9(previous page). Here, f_{90+} and f_{90-} represent the fractional portion of domain

walls which are 90 degree(+) or 90 degree(-), assumed equivalent.

The resultant magnetization is then derived by theory to be:

$$M(H,\epsilon)-M(H)=(2RHH_{\epsilon}+H_{\epsilon}{}^{2}R)f_{90+} \qquad 2\text{-}27$$

It is the purpose of this project, then, to investigate a similar result when stress is applied and also released in tension/compression cycles. The next section will describe the experiments in which the theory described here is applied for analysis of the data taken.

III. THE EXPERIMENTS

The experiments were carried out with two sample rods, one each of HY100 and HY130 ship steels. Each of these rods was one centimeter in diameter and approximately thirty centimeters long. Each rod was wound with 1010 turns of fine insulated wire to create the B-coil. The number of turns was checked by calculating the theoretical resistance and then measuring it using the voltage measured across the wire ends.

3-1 Strain Gages

Strain gages were applied directly near the ends of the rod samples. The gage factor, F_g, was defined by the manufacturer to be 2.00 within one per cent. Stress is defined to be:

$$\sigma = F/A \qquad 3\text{-}1$$

where F is the force exerted uniaxially on the rod and A is the cross-sectional area of the sample. This causes strain:

$$\epsilon = \Delta l/l = \sigma/Y \qquad 3\text{-}2$$

where l is the length of the sample and Y is Young's Modulus (2.0×10^{11} N/m^2 for steel).

From the theory, the bridge factor is defined by:

$$F_{br} = (1 + \sigma_p)/2 \qquad 2\text{-}23$$

where σ_p is Poisson's ratio for steel(0.290).

Therefore,

$$F_{br}=.645$$

Returning to the original equation, the difference between the voltage with and without force applied can now be calculated:

$$\Delta V=V_0 F_{br} F_g \epsilon \qquad 2-22$$

The strain gages were calibrated using a known DC uniaxial load of 100 lbs. The applied voltage, V_0, for the calibration was 7.7 volts, resulting in an expected ΔV of 6.2 microvolts per kilogram or 2.81 microvolts per pound. The inaccuracy in measurements was approximately five per cent.

The sources of error were investigated and the major contribution was found to be voltage drift. With an input of 7.7 volts, the output voltage was measured as a function of time. The results were plotted and a time constant of approximately fifteen minutes was measured. This result indicated that measurements of strain voltage should be made after a period of time greater than fifteen minutes or simply as finite changes in short time periods. The second method was used for the remainder of the experiments. In addition, the function generator and X-Y plotter were calibrated, yielding an uncertainty of approximately one per cent each.

3-2 The Circuit

The integrator, for integration of the B-coil voltage, was then constructed. The integrator was calibrated in order

Figure 10 --INTEGRATOR CALIBRATION

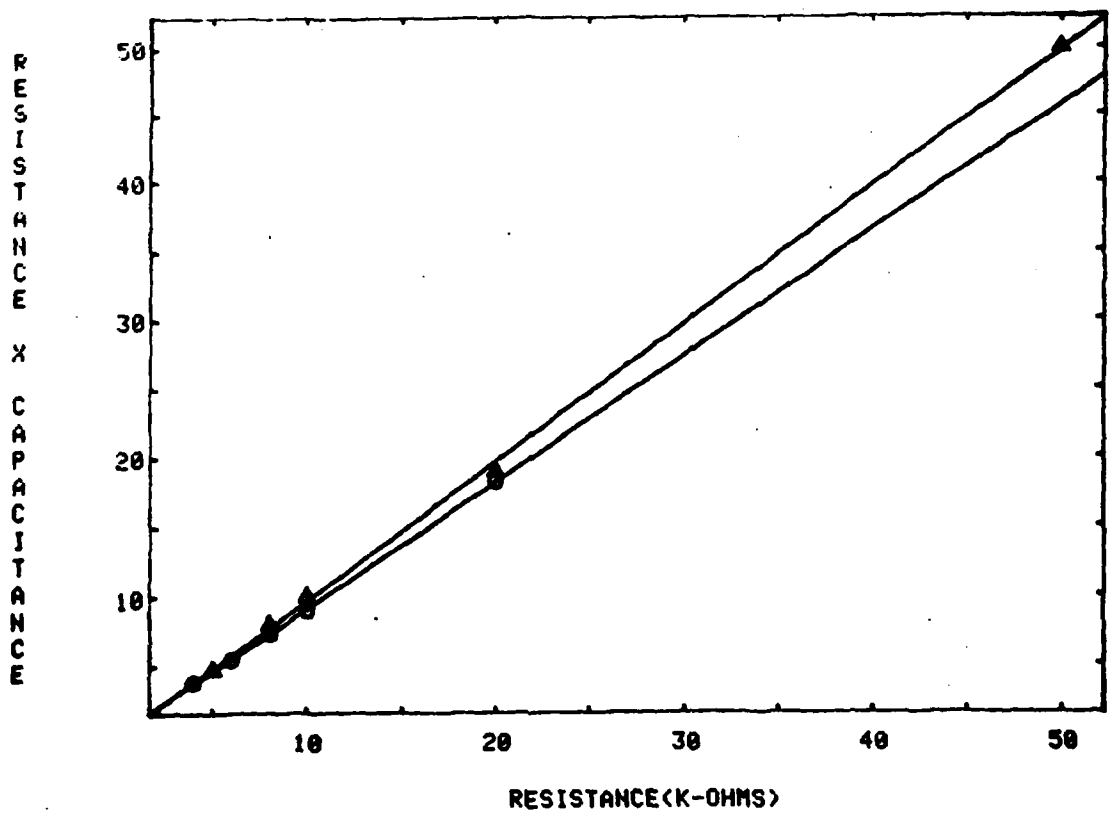

to find the proper value of the capacitor used, with a manufacturer's stated value of .999 microFarad. The integrator was calibrated using a ten millivolt DC input and then a one Hertz AC input. Using several values of resistance across the integrator, the relationship between the resistance and the time constant, RC(in milliseconds), was plotted for both of these calibrations(Figure 10). For the ten millivolt DC input (Δ), the capacitance(slope of R vs. RC) was found to be 1.013 microFarads. For the one Hertz AC input(⊙), the

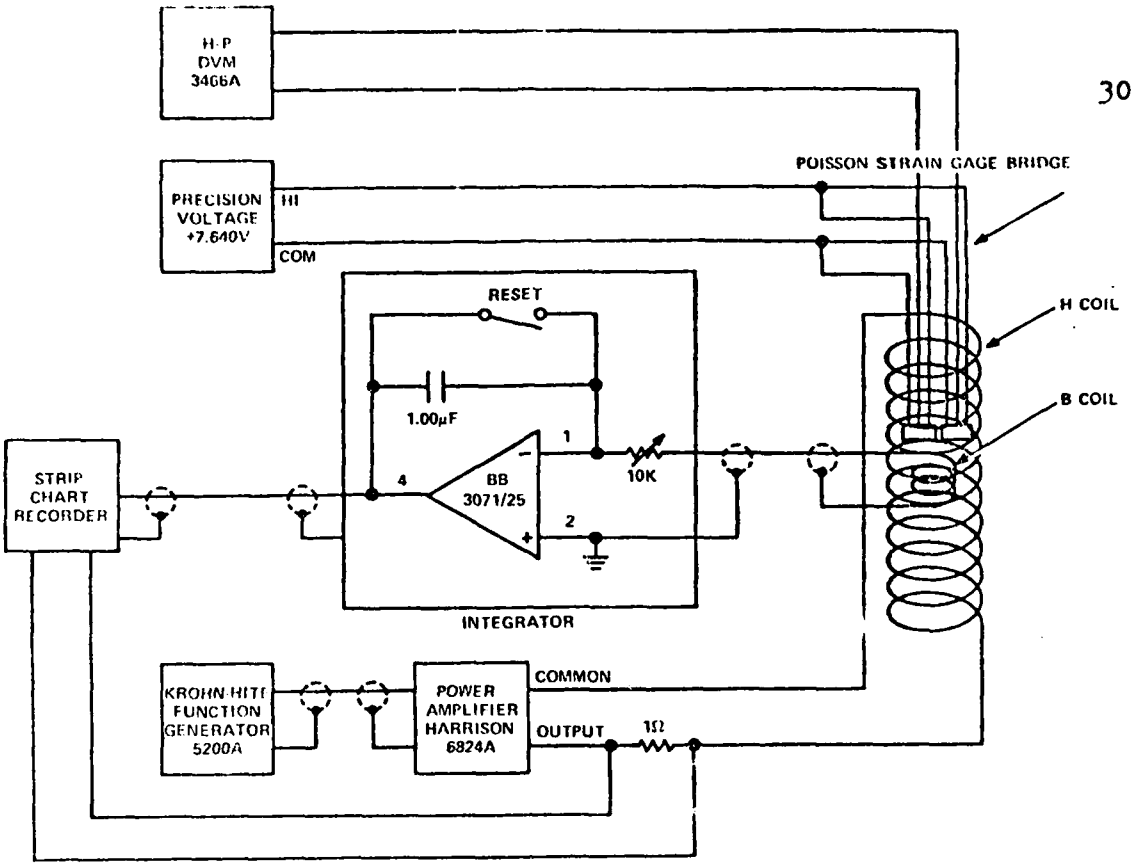

Figure 11 ---Circuit Diagram for Measurement of Strain and Magnetic Field

capacitance was found to be .913 microFarad. Considering the accuracy of the equipment used for this calibration, it was decided that a value of one microFarad would be used for the capacitance of the integrator. In addition to the capacitance measurement, the intercept of the resistance axis was used to estimate the internal resistance of the integrator. The internal resistance was found to be less than 300 ohms, which is small compared to the ten k-ohms applied resistance used for the experiments, and it was judged negligible.

Following these calibrations, the circuit was constructed for measurement of initial permeability of the samples, in

order to confirm previous measurements. Figure 11(previous page) depicts the circuit used for this calculation and for subsequent experiments.

From the theory:

$$\mu_{eff}=(RCV_B d_H/N_B \mu_0 A_B i_H) \qquad 2\text{-}17$$

The current through the H-coil is measured by taking the voltage, V_H, across a precision one ohm resistor. Equation 2-5 therefore becomes:

$$\mu_{eff}=(RCR_1 d_H V_B/\pi r_B^2 N_B \mu_0 V_H) \qquad 3\text{-}3$$

where R_1=1 ohm. Thus:

$$\mu_{eff}=35.01\ V_B/V_H \qquad 3\text{-}4$$

Therefore, by measuring the integrated B-coil voltage and the voltage across the precision one ohm resistor, the effective permeability can be measured.

3-3 The Magnetometer

From previous experiments, the permeability of HY100 is approximately 80 and that of HY130 is approximately 100(4). Therefore, it was possible to confirm which rod was made of which steel type. In order to determine the permeability in the absence of an offset field, it was necessary to place the sample rods in zero field, which was accomplished by first removing all apparatus from the table to be used for the experiments. A Schonstedt Heliflux Magnetometer was then used to find the orientation perpendicular to the local

Figure12-- EARTH'S FIELD ALONG THE APPARATUS

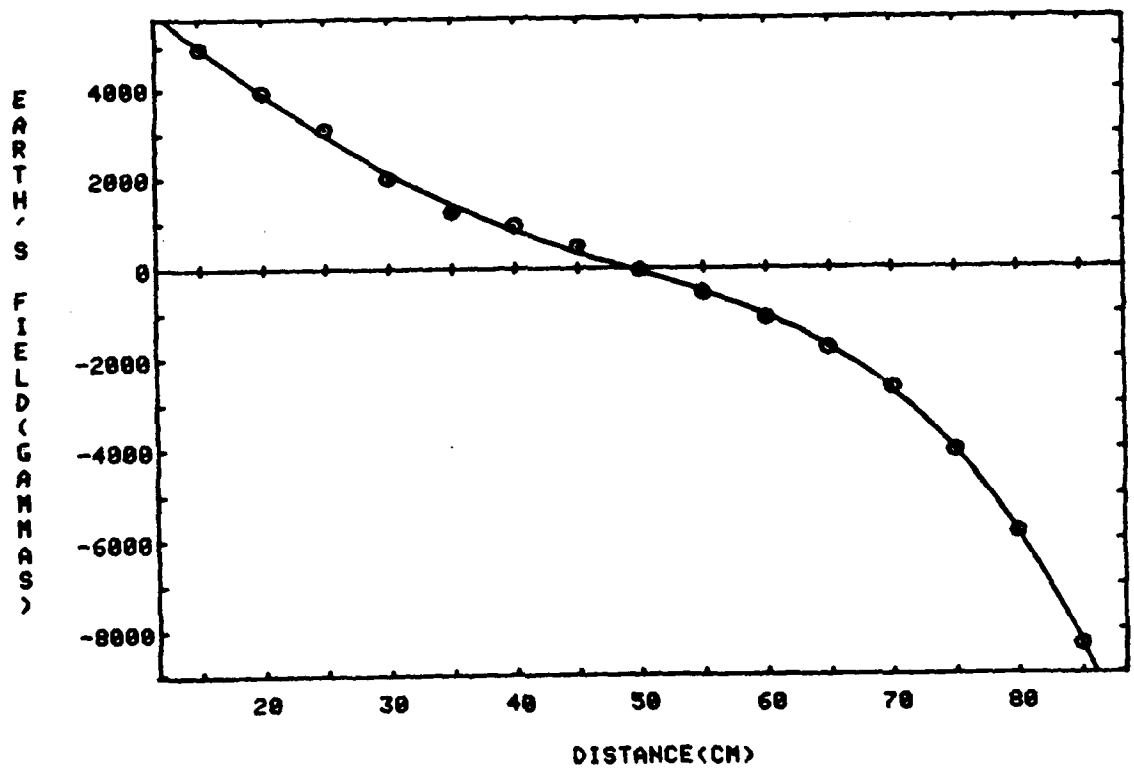

magnetic field and then the H-coil and B-coil were placed parallel to the probe. A variation of approximately $\pm$50 gamma(10^{-9} Tesla) was experienced from day to day and changes of $\pm$5 gamma were experienced when metal doors along the laboratory corridor were opened or closed.

The magnetometer was also used to find the characteristic field along the apparatus(Figure12). These measurements were taken along a straight line parallel to the probe's zero field orientation. It was found that objects containing iron affected the magnetometer reading at distances closer

than five feet from the probe, but otherwise the effect was negligible. In addition, it was discovered that an iron support column stands beneath the floor near the table where measurements were to be taken. This made the laboratory less than ideal for magnetization experiments, but it was sufficiently far from the table so as not to be detrimental to results.

All objects containing iron were placed as far from the apparatus as possible for minimal effects. The center of the B-coil, as well as the sensor element of the magnetometer probe, were secured at the zero point depicted in Figure 9.

3-4 Demagnetization

The next step was the demagnetization of the samples. There are two methods of demagnetization. In the first method, the specimen is heated to a very high temperature and then cooled in the absence of a magnetic field. In the second method, and the one used in these experiments, the specimen is magnetized by an alternating magnetic field and then the field is gradually decreased to zero in amplitude. This method decreases the size of domains in order to reduce the magnetostatic energy. This process would continue to reduce the domain size except that a certain amount of energy is necessary to form the wall between domains(2).

It was found that the demagnetization proceeded more effectively when the frequency of the field of approximately 4000 amperes per meter(50 öersteds) was slowly increased from

Figure 13---Vibration-Simulation Apparatus

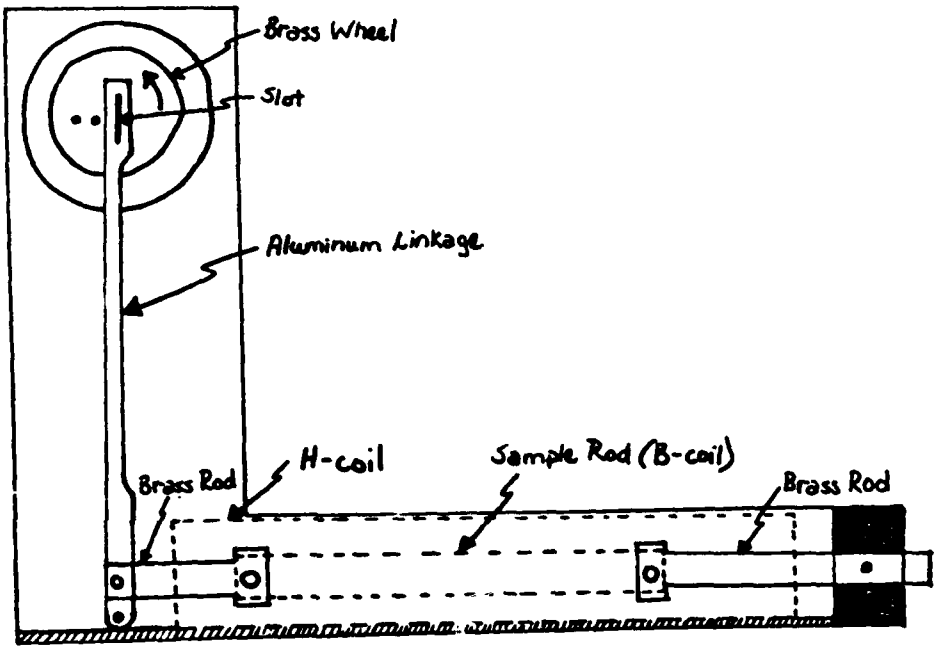

two to thirty Hertz before the amplitude of the field was decreased to zero. Fine adjustments of the DC offset within the function generator were also necessary in order to precisely zero the average field along the rods.

3-5 Vibration-Simulation Apparatus

The next step was to complete construction of the non-magnetic apparatus which would be used for simulation of vibration and to mount it on the table within the laboratory. Figure 13 is a simplification of the apparatus used. Small pins set off-center on the wheel, slide in the slot of the

Figure 14-- STRAIN VS. DRIVE ANGLE(HY100)

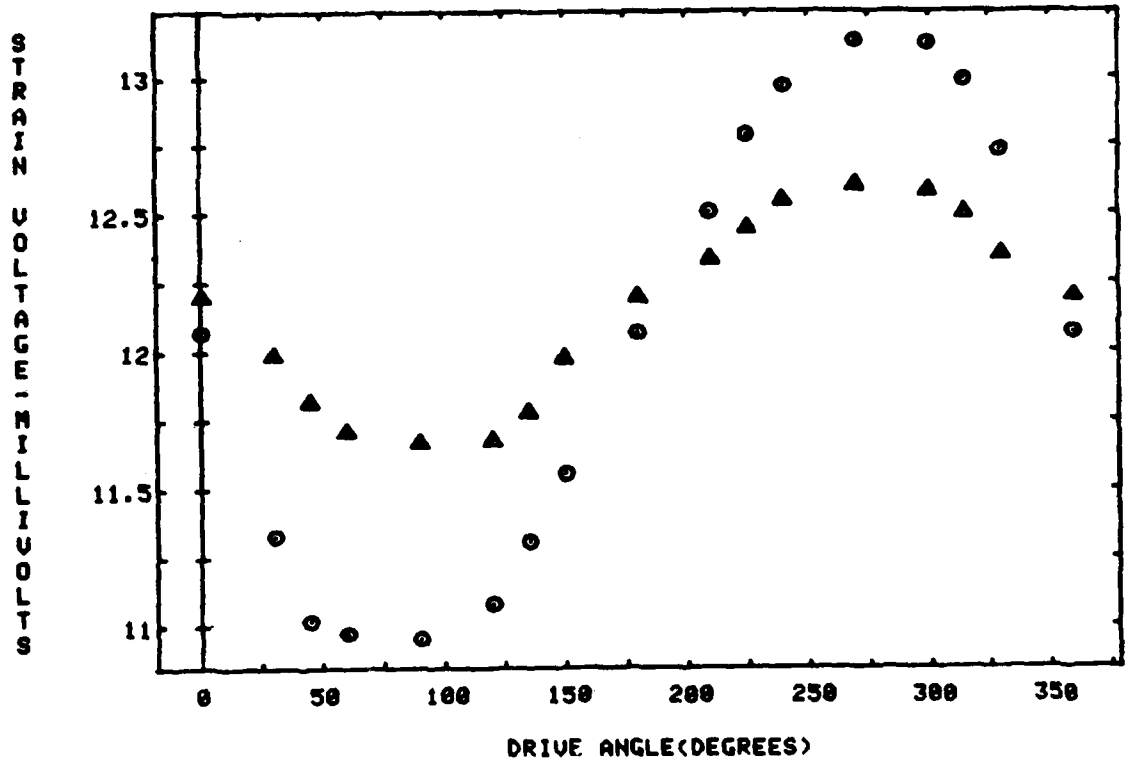

lever arm on the left. As the wheel is turned, the rotary motion is converted to transverse stress at the bottom of the linkage. The bottom of the linkage is secured to the base of the apparatus with a pin. The sample rods are inserted between two brass rods within the H-coil. The brass rod on the right is fixed securely by a pin which goes through the base of the apparatus. The sample, then,is secured to both brass rods using stainless steel pins. The brass rod on the left is attached to the linkage with a stainless steel pin.

Figure 15--STRAIN VS. DRIVE ANGLE(HY130)

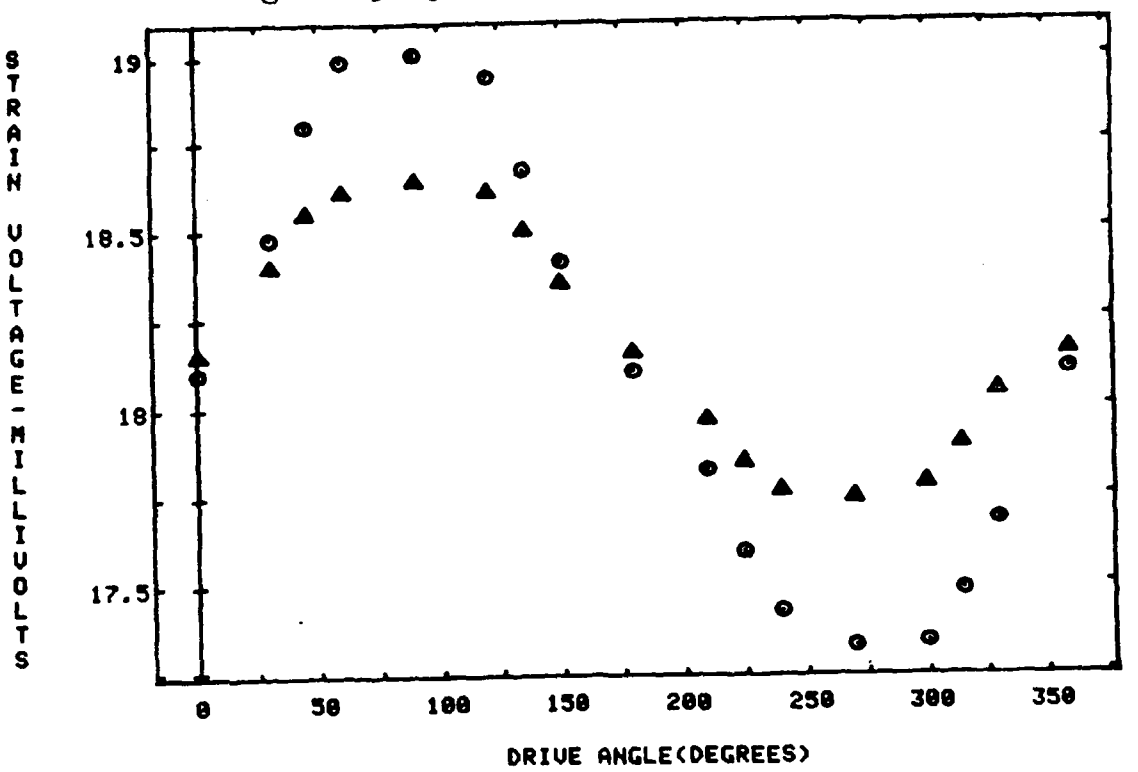

Therefore, the samples experience alternating compression and tension as the wheel turns. Plotting these cycles using the strain gages(Figures 14 and 15), a sinusoidal process is observed. Figure 14 shows the results for HY100. The first action was that of compression beginning, in this case, with a negative slope. A zero degree drive angle indicates equilibrium and a ninety degree drive angle indicates maximum compression. As can be seen, two stress magnitudes were applied, one of approximately fifty microstrains in both tension and compression and the other of approximately

one hundred microstrains. Figure 15 shows the results of the same tests using the rod made of HY130 steel. Compression was again the initial action, but this time resulted in an initial positive slope of the curve. This result is due simply to the reversed polarity of the strain gage circuit. Results also showed the HY130 steel rod began with a higher voltage at equilibrium, indicating greater initial imbalance in the resistance of the four gages in the circuit. Finally, both graphs show a slightly larger strain in compression than in tension, but insufficient to affect the experiments which were performed.

The apparatus was then bolted to the table in line with the probe oriented at zero field, such that when the sample rods were placed inside the apparatus, the center of the B-coil was at zero field, minimizing the effects of the earth's field on it.

3-6 Short-term Experiments

The apparatus was then ready for experiments with and without applied stress. Using the circuit previously described, V_H vs. V_B curves were made at various applied field amplitudes. On the X-Y plotter the B-field voltage corresponded to the X-axis and the H-field voltage corresponded to the Y-axis. These measurements were taken at fields between approximately ten and eighty amperes per meter, forty amperes per meter being the approximate field of the earth. For each field amplitude, plots were made with no stress applied, then with stress of approximately fifty and one hundred

microstrains. Typical results are graphically displayed in Figure 16.

For the fifty microstrain amplitude, a 1/8 horsepower

Figure 16--Typical V_H vs. V_B Plots(ϵ =0, ϵ =50 $\mu\epsilon$)

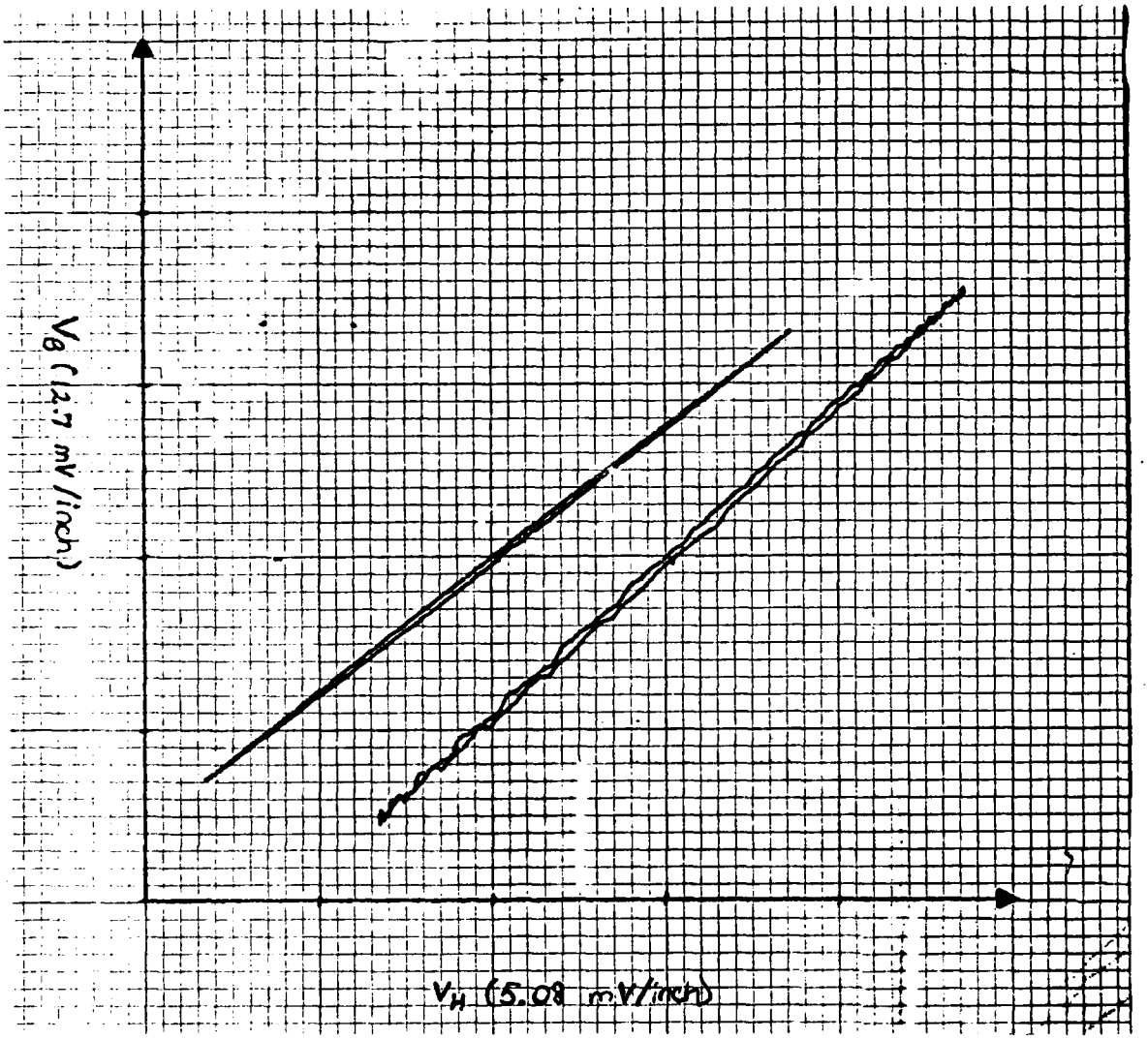

variable speed AC motor was connected to a shaft which turned the wheel imparting the stress. This motor allowed the tests to be run at both four and five cycles per second

for observation of frequency dependence: there was none.

For the one hundred microstrain application the motor was not powerful enough to turn the wheel. Therefore, a handcrank was used, which allowed a fairly steady three cycles per second stress application. Figure 16 shows a definite change in slope, dB/dH, for both stress applications. Analysis will be presented in the next section.

One of the problems encountered in performing these tests was the observable(Figure 16) oscillation in the magnetization with stress cycles. Hard perm in the rods(that remanent magnetization which can not be "shaken loose" by the strength of fields applied in demagnetization) is unresponsive to the stress cycles. Soft perm, on the other hand (that magnetization which <u>can</u> be changed by the fields and stresses applied),balances hard perm in the unmagnetized state and displays significant modulation during stress oscillations. The soft perm was removed by magnetizing until response to stress oscillations reached a minimum. The balance point for the HY100 sample rod was approximately 77 Gauss and for the HY130 sample, 234 Gauss. These values indicate, then, the presence of hard perm in the HY100 steel and a larger amount of hard perm in the HY130 steel.

3-7 Long-term Experiments

Following these tests, the effect of long-term cyclic stress was investigated. For these tests, the V_H vs. V_B curves could not be used since voltage drift would become a major factor after long periods of time. Instead, the

Figure 17--MAGNETOMETER CALIBRATION

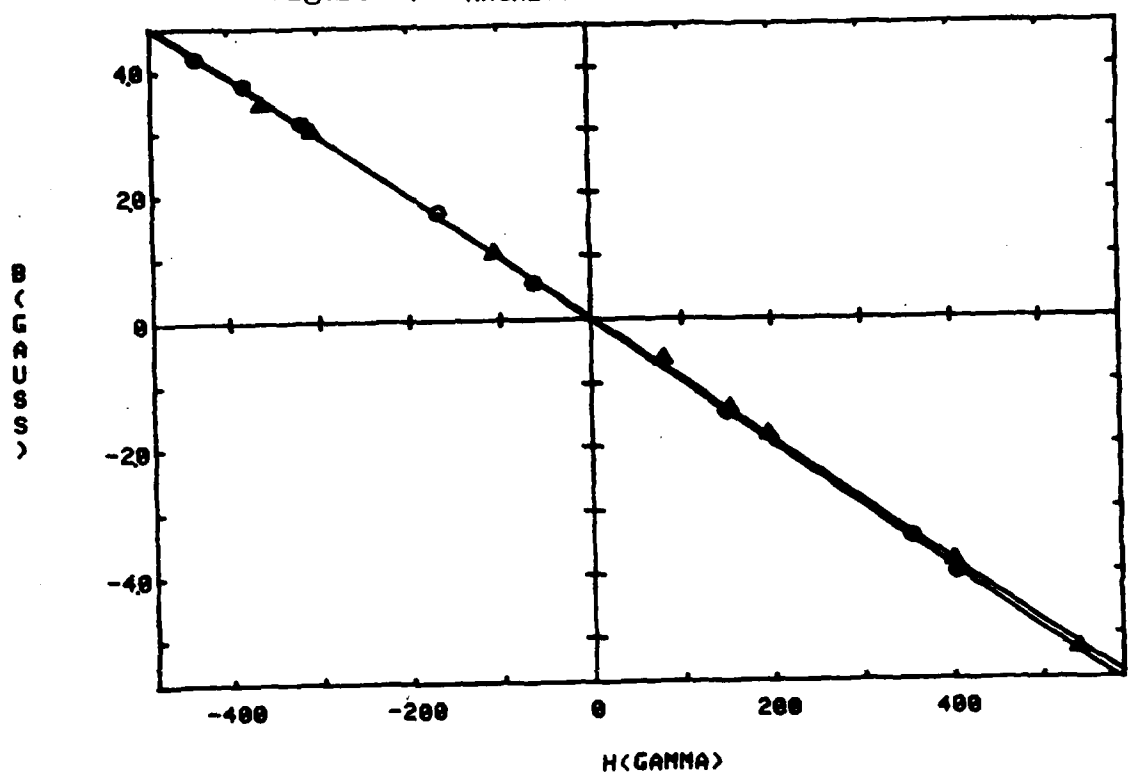

objective was to apply DC H-fields and read changes in magnetization on the Schonstedt Heliflux Magnetometer with vibration.

In order to interpret the magnetometer as a magnetization detector, it was calibrated using rods in varying fields, comparing B-coil readings with magnetometer changes. The results of these calibrations are shown graphically in Figure 17. The points surrounded by triangles indicate results for the HY100 steel rod and the circled points indicate the results for the HY130 steel rod, both showing agreement within a few per cent.

The HY100 steel rod was used for these cyclic stress tests. The fifty microstrain stress was applied in zero field and with an applied field at four cycles per second for 10,000 cycles. The one hundred microstrain stress was also applied in zero field and with an applied field. These tests were done with the handcrank, again at approximately three cycles per second, for 2000 cycles. Measurements were made at different intervals during the repeated stress cycles.

The results and analysis of these experiments will be dealt with in the next section.

IV. RESULTS AND DATA ANALYSIS

In this section, the experimental results of the AC field cycles with and without vibration applied, and the long-term changes in magnetization due to repeated stress cycles, will be analyzed.

4-1 Short-Term Effects

From the V_B vs. V_H plots described in the experiments, the susceptibility and field were calculated and plotted. Figure 18(next page) shows the results for the HY100 steel sample rod. The H-field was calculated in amperes per meter, forty amperes per meter being the approximate field of the earth. Both the susceptibility and the H-field were corrected for the demagnetizing factor, which is approximately 1/400 for both rods. The value for permeability of HY100 which was used for the correction was 80.

The circled points show the results when no stress was applied. The graph shows a linear increase in the susceptibility as the field within the sample rod increases. The initial susceptibility, χ_i, which is the susceptibility at zero field, was found to be 76.9, which agrees with results from tests performed in FY1978 by Professor Carl S.Schneider at DTNSRDC, Annapolis(4).

Those points surrounded by triangles show results when a stress of forty-seven microstrains was applied. The initial susceptibility and all subsequent susceptibilities are higher than that found at equivalent fields with no stress applied. The curve is again linear and has

Figure 18--SUSCEPTIBILITY VARIATION W/STRESS AND FIELD (HY100)

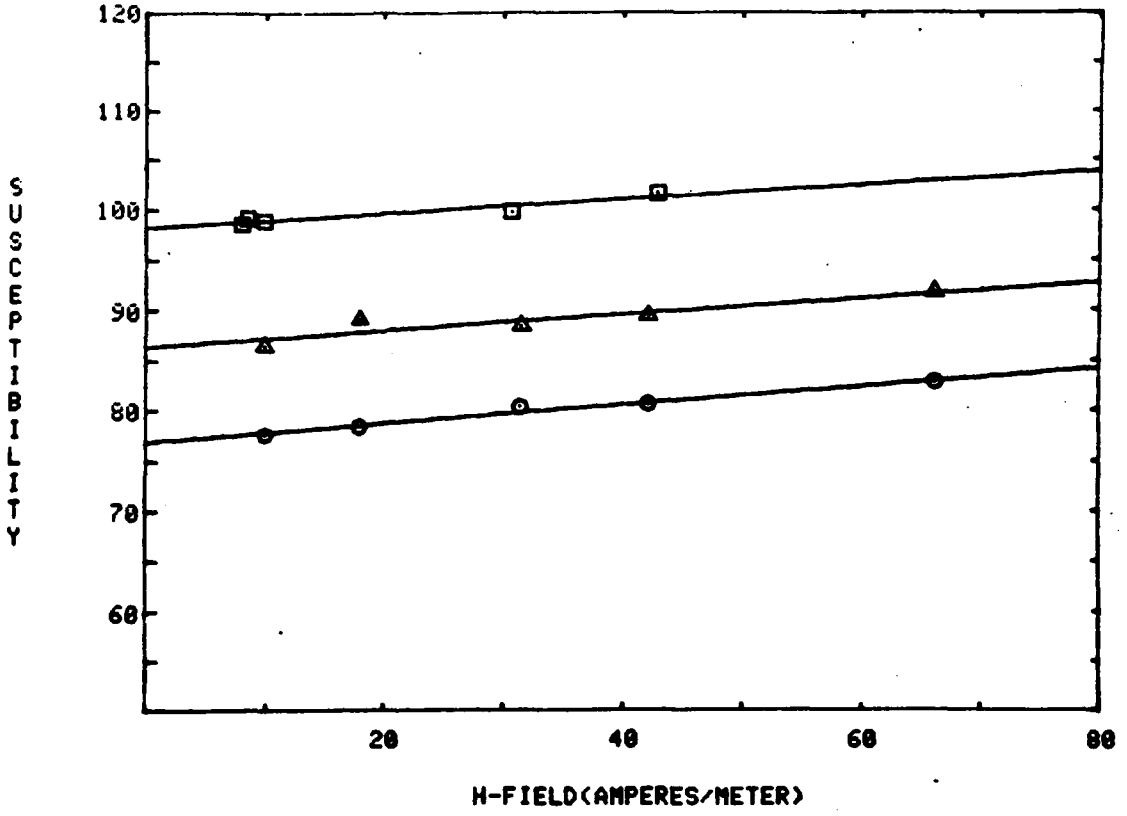

a similar slope to the first set of points. The data for this stress level was taken at both four and five Hertz stress cycles, with similar results, showing no frequency dependence.

Those points surrounded by squares are those with 110 microstrain stress cycles applied. Again, results showed a higher initial susceptibility, as well as increased susceptibility at all other points. The relationship is again linear and has a similar slope to the other two sets of data. These experiments were performed at three

Figure 19---SUSCEPTIBILITY VARIATION W/STRESS AND FIELD (HY130)

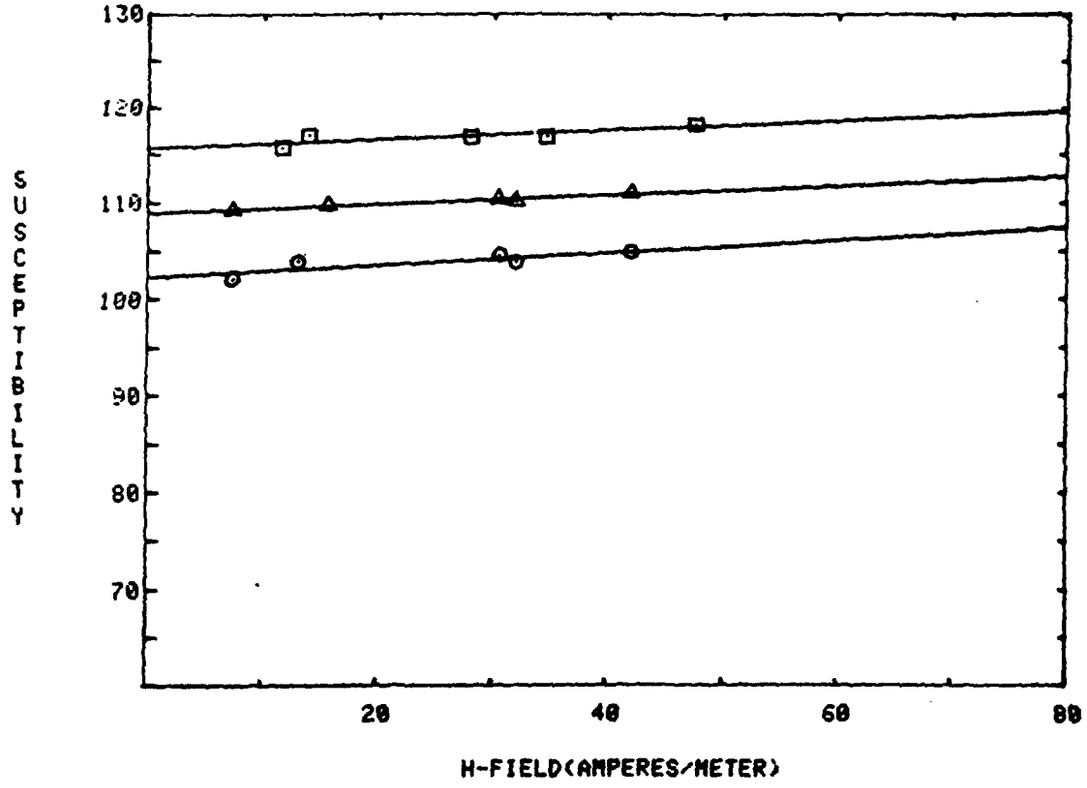

Hertz stress cycles using a hand crank.

Figure 19 shows the results of the same experiments using the HY130 steel sample rod. Without strain, the initial susceptibility was 102.3, again agreeing with previous research. The same linear relationships as those for the HY100 steel were found. The susceptibility of the HY130 steel, however, was higher in all cases. For this steel, the stress amplitudes were forty-five microstrains and eighty-five microstrains. These changes in the magnitude

of the stress show that there was some breakdown in the system with repeated stress cycles. Because the fittings for the rods were made of brass, it is probable that the holes in these fittings through which pins were inserted grew larger as a result of repeated stress cycles. Therefore, movement of the rods increased and the amplitude of the strain created within them was decreased.

From these graphs we found the initial susceptibility, χ_i, for each rod and for each amplitude of strain. The results are shown in Table I below:

TABLE I

Initial Susceptibility as Function of Strain

HY100		HY130	
$\epsilon(\mu\epsilon)$	χ_i	$\epsilon(\mu\epsilon)$	χ_i
0	76.9	0	102.3
47	86.4	45	108.9
110	98.2	85	115.7

The plot of these points is shown in Figure 20(next page). A linear relationship is again observed, with similar slopes for both steel types. Looking again at Rayleigh's theory, the equation derived for stress application is:

$$M(H,\epsilon)-M(H)=(2RHH_\epsilon + H_\epsilon^2 R)f_{90+ \text{ or } -} \qquad 2\text{-}27$$

Because the susceptibility is defined as the change in magnetization with changing field, the relationship sought is:

Figure 20--INITIAL SUSCEPTIBILITY VS. STRAIN (HY100 AND HY130)

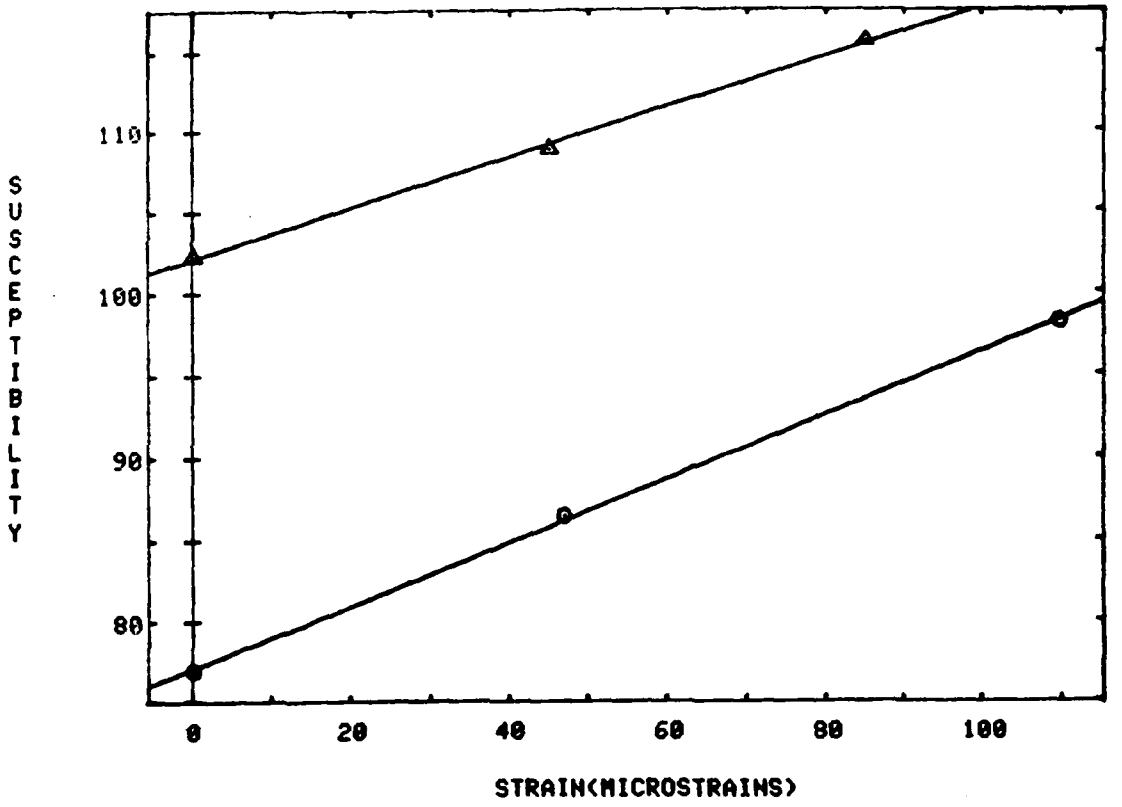

$$\chi_{eff}=M(H,\epsilon,\bar{\epsilon})/H \qquad 4\text{-}1$$

The results of the experiments conducted indicate that the quadratic term in equation 2-27 is dropped in this case, yielding a linear relationship between the susceptibility and strain, as well as field. From this work, then, the equation for the change in susceptibility with vibration is of the form:

$$\chi_{eff}=M(H,\epsilon,\bar{\epsilon})/H=\chi_i+4RfH_e \qquad 4\text{-}2$$

where the factor of four is due to two factors of two: one from the ratio of differential to normal susceptibility slope, and the other from the experimentally observed additive contributions of tension and compression to susceptibility enhancement. Expressing this enhancement empirically, we define:

$$\chi_{eff}=\chi_i+R\epsilon\alpha \qquad 4\text{-}3$$

where, for HY100, we observe from Figure 20:

$$d\chi_{eff}/d\epsilon=0.193/\mu\epsilon$$

and from Figure 18:

$$R_{100}=80\pm5 \text{ mm/A} \text{ , so } \alpha_{100}=2.41\pm.15 \text{ MA/m.}$$

For HY130, we observe from Figure 20:

$$d\chi_{eff}/d\epsilon=0.157/\mu\epsilon$$

and from Figure 19:

$$R_{130}=53\pm5 \text{ mm/a} \text{ , so } \alpha_{130}=2.96\pm.30 \text{ MA/m.}$$

The smaller difference between coefficients α (twenty per cent or just over one standard deviation) and the Rayleigh coefficients(fifty per cent or five standard deviations) suggests that α may be due purely to steel composition.

Theoretically, from equations 4-2 and 4-3:

$$\alpha=(d\chi_{eff}/d\epsilon)/R=4f(\delta H_e/d\epsilon) \qquad 4\text{-}4$$

where from equation 2-25:

$$\alpha = 4f\, d(3/2(\lambda_s \epsilon Y/\mu_0 M_s))/d\epsilon = 6\lambda_s Yf/\mu_0 M_s \qquad 4\text{-}5$$

where Y is Young's modulus(2.0×10^{11} N/m^2 for steel) and f is the fraction of domains which are responsive to stress. Thus,

$$f = \alpha\mu_0 M_s/6\lambda_s Y = 0.55 \qquad 4\text{-}6$$

where $\mu_0 M_s$ is 1.93 Teslas for HY100 and λ_s is seven microstrains for iron, but is not known for HY steels, and α_{100} is used. Since f is expected to be the fraction of domains with 90 degree walls, roughly one-half, results agree with those theoretically derived.

4-2 Long-Term Effects

Long-term effects were then plotted and analyzed. Figure 21(next page) shows the results of these tests for the HY100 steel sample. The points surrounded by squares show the results of 10,000 cycles, at a strain amplitude of approximately forty-five microstrains, in the absence of a field. Random fluctuations occur around the initial magnetization, but no change in the magnetization is observed.

The circled points show the results with an applied DC field. Again, forty-five microstrains are applied for 10,000 cycles. The intercept of the magnetometer reading axis shows the change in magnetization with one cycle.

Figure 21-----CHANGES IN MAGNETIZATION WITH CYCLIC STRESS

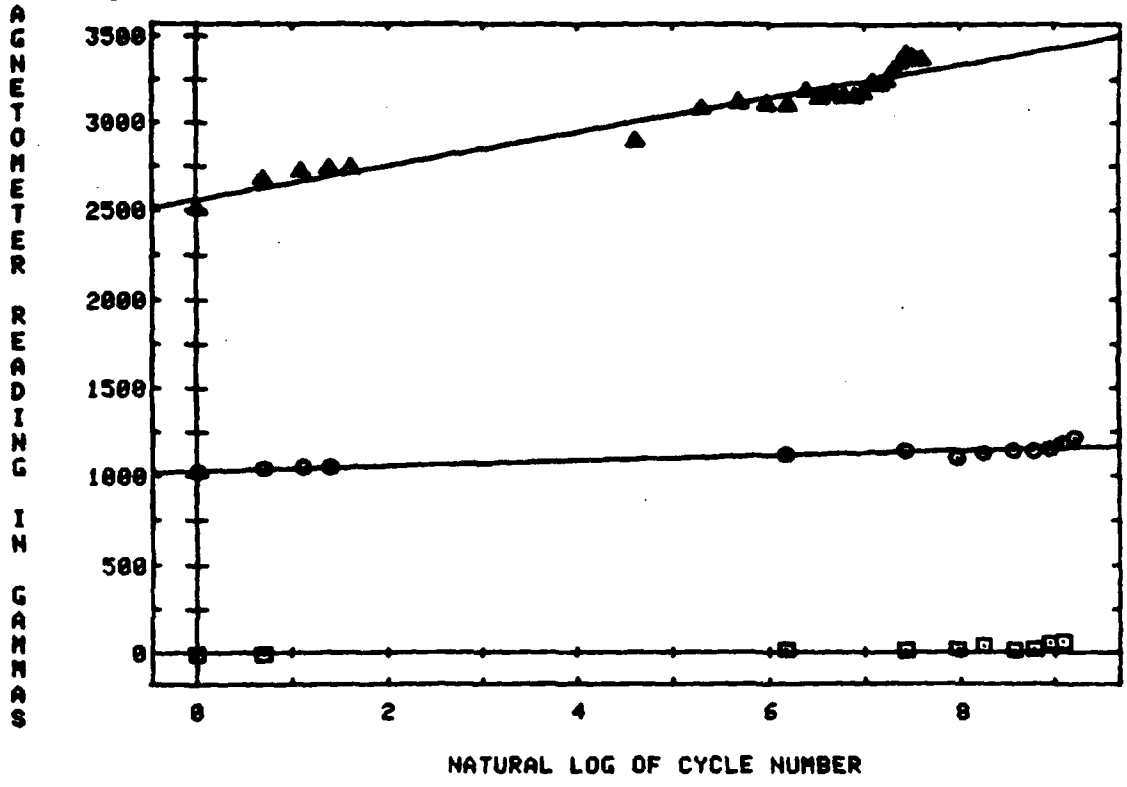

As can be seen, the largest change in magnetization occurs in this first cycle. This can be compared to the shock experiments described in the first section. When a ship's steel undergoes shock, it will also undergo a change in magnetization dependent upon the amplitude of the shock.

The 10,000 cycles applied took approximately 40-50 minutes at four Hertz, with a definite increase in magnetization over this time period. The fact that the amplitude of the stress was relatively small emphasizes the fact

that stress cycles have a major effect on a ship's magnetization during voyaging.

The points surrounded by triangles indicate changes in magnetization in the presence of a field for 2000 cycles at a strain amplitude of approximately 100 microstrains. The rise in magnetization is even more pronounced than that of the smaller stress cycles, indicating a strong dependence on strain amplitudes. Again, the intercept shows the change in magnetization over the first cycle, indicating the strong effect of this first cycle. These cycles were done by hand and were therefore not taken to 10,000 cycles, but the rising trend is obvious.

As can be seen, the results were plotted as a function of the log of the number of cycles, rather than the square root of the log, as was predicted by Néel for cyclic fields. The results of these experiments do not conclusively show that either of these dependencies is correct or incorrect. The work done by Van Dang in this area is also questionable. Further tests must be made under more ideal conditions, in order to clarify this dependence.

It is obvious, however, that there is a definite rise in magnetization in the presence of a field after long-term cyclic stress. If, after only forty minutes at four Hertz, there is a noticeable change in the magnetization, the changes observed after a year or more would be quite marked. In the next section, conclusions will be drawn from the experimental results and suggestions for further research will be made.

CHAPTER V

DISCUSSION

The results of this research indicate several important conclusions. First, the ability to simulate voyage effects, both vibration and shock, is possible through the methods described. Therefore, similar experiments using more submarine-like models may lead to important conclusions for naval applications.

The increased rise in susceptibility in the presence of cyclic stress has been shown quantitatively(for the first time) in small fields, such as those of the earth. In addition, the higher initial susceptibility caused by the application of stress is an important parameter for naval vessels. By knowing the initial susceptibility, the induced magnetization can be more accurately measured and the ship can be permed to balance the magnetization. In this manner, the ship may become magnetically undetectable.

For the magnetic induction vs. field, the frequency of the stress cycles had no effect on the results. In addition, nothing in the theory indicates that there is a frequency-dependent effect. However, the change in magnetization was found to be dependent upon the number of cycles. Cyclic stress was applied for 10,000 cycles, with a noticeable increase in magnetization in the presence of a DC field.

This marks the first time stress-induced reptation was observed quantitatively, and is the first time reptation was measured below one-third the coercive force, the lower limit for Van Dang in 1959. The effect was even more marked at one hundred microstrains than at fifty microstrains. The question of dependence on log n(number of cycles) or $(\log n)^{\frac{1}{2}}$ was not resolved, but further experiments will provide the answer. Finally, the fraction of domains which respond to stress was found to be about one-half. This indicates a balance between 90 degree and 180 degree walls.

For further experiments, a hollow cylinder may be used and also a 1/100-scale model submarine, which is available on loan from the Naval Ships Weapons Center, White Oak, Maryland. However, the equipment used for these experiments will have to be more sophisticated than that which is presently available. In addition, vibration amplitude measurements with strain gages on submarines themselves would provide important information for analysis of the field component of reptation. The submarine hull undergoes biaxial strain in comparison to the uniaxial strain experienced by the sample rods. This parameter must also be taken into account.

Other effects related to voyaging must also be analyzed in future research. Most of the subjects which were not addressed in this work are related to time-effects. This includes the effects of temperature, as well as eddy currents. Eddy current effects, which are small for low frequency fields, such as those used for these experiments, cause the magnetic

induction to decrease from the surface to the interior, thus creating a change in the overall magnetization(10). The area of "magnetic viscosity(11)" involves the initial susceptibility and is quite temperature-dependent. It has been found that there is a time decrease in susceptibility, which is observed only at low field values, such as those experienced on the earth. This thermal time-effect must be analyzed for more accurate prediction of voyage effects.

Finally, experiments must be conducted with samples of HY80 steel, for which no data was taken. Problems in attaching the HY80 sample rod to the vibration apparatus caused it to become unusable. HY80 steel is that steel from which submarines are made. Professor Carl S. Schneider(4), who worked with HY80 using static stress, found the susceptibility of this steel to be similar to that of HY100. Therefore, the results of experiments with HY100 are a strong indication of results expected using HY80. However, it is still important that these experiments be completed.

In conclusion, by conducting experiments in a similar manner with models which more closely represent submarines, results may be extrapolated to actual submarines. Through the ability to predict changes in magnetization due to certain variables, it may be possible to discover certain maneuvers, such as changes in direction, depth of voyaging, or changes in internal stress, which could return the ship to a well-known magnetic state, such that its magnetization can be accurately controllable.

REFERENCES

1. Sir James Alfred Ewing, Magnetic Induction in Iron and Other Metals(D. Van Nostrand, New York, London, 1892).

2. Soshin Chikazumi, Physics of Magnetism(John Wiley and Sons, Inc., New York, London, Sydney, 1964).

3. John R. Reitz and Frederick J. Milford, Foundations of Electromagnetic Theory(Addison-Wesley Publishing Company, Reading, Mass., Palo Alto, London, Don Mills, Ontario, 1967).

4. C. S. Schneider, "Magnetoelastic and Vibration Effects of the Ultraservice Steels."(David W. Taylor Naval Ship Research and Development Center, Maryland, 1979),PAS 79-4.

5. William Fuller Brown, Jr., "Irreversible Magnetic Effects of Stress," Phys. Rev.,75(1949),pp. 147-154.

6. R. R. Birss, "Magnetomechanical Effects in the Rayleigh Region," IEEE Transactions on Magnetics(1971),pp. 113-133.

7. N. Van Dang, "Resultats experimentaux sur la reptation et la bascule dans les cycles d'hystereis," J. Phys. Radium, 20(1959),pp. 222-228.

8. L. Neel, "Action des champs magnetiques successifs de caractere aleatoire sur l'aimantation des substances ferromagnetiques," C. R. Acad. Sci., 244(1957), pp. 2441-2446.

9. Charles Kittel, "Theory of Long Period Magnetic Relaxation," Phys. Rev., 69(1946), pp. 640-644.

10. Richard M. Bozorth, Ferromagnetism(D. Van Nostrand, Toronto, New York, London, 1951).

11. J. L. Snoek, "Time Effects in Magnetization," Physica, 5(1938), pp. 663-688.

12. Paul A. Tipler, Physics(Worth Publishers, Inc., New York, 1976).

13. H. Ziljstra, "Experimental Methods in Magnetization," 9 of Selected Topics in Solid State Physics. Ed. E. P. Wohlfarth. New York: Wiley and Sons(1967), pp. 145-147.

14. O. Yamada, "Rise in Magnetization due to Stress," Electrical Engineering in Japan, 88(1968), pp. 1-6.

15. R. Becker and W. Doring, Ferromagnetismus(Springer Verlag, Berlin, 1939).

16. C. S. Schneider. Annual Report: FY1980. DTNSRDC, Annapolis(in progress).

17. C. C. Perry, H. R. Lissner, The Strain Gage Primer, Second Edition(McGraw-Hill, New York, 1962).